Electronic Supplementary Information for

Visible-light induced overall water-splitting photocatalyst : conduction band-controlled silver tantalate

Lei Ni,[a,b] Momoko Tanabe,[c] and Hiroshi Irie*[a,d]

[a] Clean Energy Research Center, University of Yamanashi, 4-3-11 Takeda, Kofu, Yamanashi 400-8511, Japan.
Fax: +81 55 220 8092; Tel: +81 55 220 8092; E-mail: hirie@yamanashi.ac.jp
[b] Center for Instrumental Analysis, University of Yamanashi, 4-3-11 Takeda, Kofu, Yamanashi 400-8511, Japan
[c] Faculty of Engineering, University of Yamanashi, 4-3-11 Takeda, Kofu, Yamanashi 400-8511, Japan
[d] Japan Science and Technology Agency, CREST, 5 Sanbancho, Chiyoda-ku, Tokyo 102-0075, Japan

Contents

ESI-1) Detailed sample preparation of $AgTa_{1-x}Nb_xO_3$ (x = 0, 0.2, 0.3, 0.4, and 1).

$AgTa_{1-x}Nb_xO_3$ (x = 0, 0.2, 0.3, 0.4, and 1) powdered photocatalysts were synthesized using a hydrothermal method. Briefly, stoichiometric amounts of silver nitrate ($AgNO_3$, 1 mol/L, Kanto Kagaku), tantalum ethoxide ($Ta(OC_2H_5)_5$, purity 99.98 %, Aldrich), and niobium ethoxide ($Nb(OC_2H_5)_5$, purity 99.95 %, Aldrich) were dissolved in 180 mL distilled water and the resulting mixture was transferred to a 300-mL Teflon-lined stainless steel autoclave. A typical amounts of starting materials, $AgNO_3$, $Ta(OC_2H_5)_5$, and $Nb(OC_2H_5)_5$ for $AgTa_{1-x}Nb_xO_3$ (x = 0.3) are 3.517×10^{1} mL, 1.000×10^{1} g, and 3.357 g, respectively. After heating at 180 °C for 48 h, the suspension was centrifuged and the obtained precipitates were washed with a sufficient amount of distilled water. The centrifugation and washing procedures were repeated four times, and the obtained precipitates were dried at 80 °C on a hotplate, and then calcined at 850 °C for 24 h. For the grafting of NiO as a co-catalyst onto $AgTa_{1-x}Nb_xO_3$, and an amount of nickel nitrate hexahydrate ($Ni(NO_3)_3\cdot 6H_2O$, purity 98.0 %, Kanto Kagaku), as the source of NiO, that gave a weight fraction of NiO relative to $AgTa_{1-x}Nb_xO_3$ of 5×10^{-3} (0.5 wt%) was first dissolved in 2 mL distilled water in an agate mortar. One gram of $AgTa_{1-x}Nb_xO_3$ powder was then added to the $Ni(NO_3)_3\cdot6H_2O$ solution, which was then mixed manually using a pestle. The formed residues were heated at 300 °C for 1 h and subsequently treated in 50 mL HNO_3 solution (5 M) for 10 min. The powders were then washed with a sufficient amount of distilled water and dried at 50 °C in an oven.

ESI-2) Detailed characterization procedures, XRD, UV-vis, SEM, BET, and photocatalytic water-splitting tests.

The crystal structures of the prepared powders were determined by X-ray diffraction (XRD, Panalytical PW-1700). UV-visible absorption spectra (UV-vis) were obtained by the diffuse reflection method using a spectrometer (V-650; JASCO) and $BaSO_4$ as a reflectance standard. A scanning electron microscope (SEM, S-4500; Hitachi) was used to observe the prepared photocatalysts. Brunauer-Emmett-Teller (BET) surface areas were determined using a nitrogen adsorption apparatus (Micromeritics, TriStar 3000; Shimadzu).

Photocatalytic overall water-splitting tests were conducted in a gas-closed circulation system. Photocatalyst powders (60 mg) were suspended in 10 mL water using a magnetic stirrer. Argon gas (50 kPa) was introduced into the system after repeated deaeration to a final pressure of 2.5 Pa. Light-emitting diode (LED) lamps with wavelengths of 405 nm (LEDH60-405, Hamamatsu Photonics) and 420 nm (LEDH60-420, Hamamatsu Photonics) were used for visible light irradiation of the system. The amounts of evolved H_2 and O_2 were monitored using an online gas chromatograph (GC-8A; Shimadzu).

ESI-3) XRD, SEM, and BET characterization results.

Figure S1a and S1b show the observed XRD patterns of $AgTa_{1-x}Nb_xO_3$ (x = 0, 0.2, 0.3, 0.4, and 1) and the reported XRD peaks of $AgTaO_3$ (ICSD #98-004-7405). $AgTa_{1-x}Nb_xO_3$ (x = 0.2, 0.3, and 0.4) appeared to have a single phase of $AgTaO_3$. In addition, the XRD peaks did not shift regardless of x value up to 0.3, as shown in Figs. S1c–S1f. As the effective ionic radii of Ta^{5+} and Nb^{5+} (six-coordination) are the same (0.064 nm; Shannon, R. D.; Prewitt, C. T., *Acta Cryst. B*, **1969**, *25*, 925-946), it was likely that the peak shifts wre not be observed. Thus, Nb ions were successfully incorporated at Ta sites. In the case of $AgTa_{1-x}Nb_xO_3$ (x = 0.4), the XRD peaks shifted to a higher angle, compared to $AgTa_{1-x}Nb_xO_3$ (x = 0, 0.2 and 0.3), as shown in Figs. S1c–S1f. The observed peak shifts were not likely the result of the difference in the ionic radii. At present, the peak shift to a higher angle with x = 0.4 is not clear, however, it could be attributed to the existence of defects (oxygen vacancy and so on), resulting in the smaller lattice conctants.

In the case of $AgNbO_3$, it did not have a single phase of $AgNbO_3$, with small impurity peaks at ~ 30° appeared. The preparation conditions for obtaining the single phase of $AgNbO_3$ might be different from those for $AgTaO_3$; however, the preparation conditions of $AgNbO_3$ were not optimized due to the following three reasons: 1) the impurity peaks were small, 2) the band-gap obtained by UV-vis spectroscopy, which was presented in Fig. 2, was the same (2.8 eV) as the reported value, and 3) it was not necessary to measure the water-splitting reaction.

SEM images of the $AgTa_{1-x}Nb_xO_3$ powders after calcination at 850 °C were taken to compare their crystallite sizes and surface areas (Fig. S2). The crystallite sizes of the as-prepared $AgTa_{1-x}Nb_xO_3$ samples ranged from several hundred nanometers to sub-micron meter aggregated forms. This result was not unexpected because the powders were subjected to calcination at 850 °C for 24 h. In addition, the surface area of the prepared material was low, ranging from ~ 1 to 2 m^2/g.

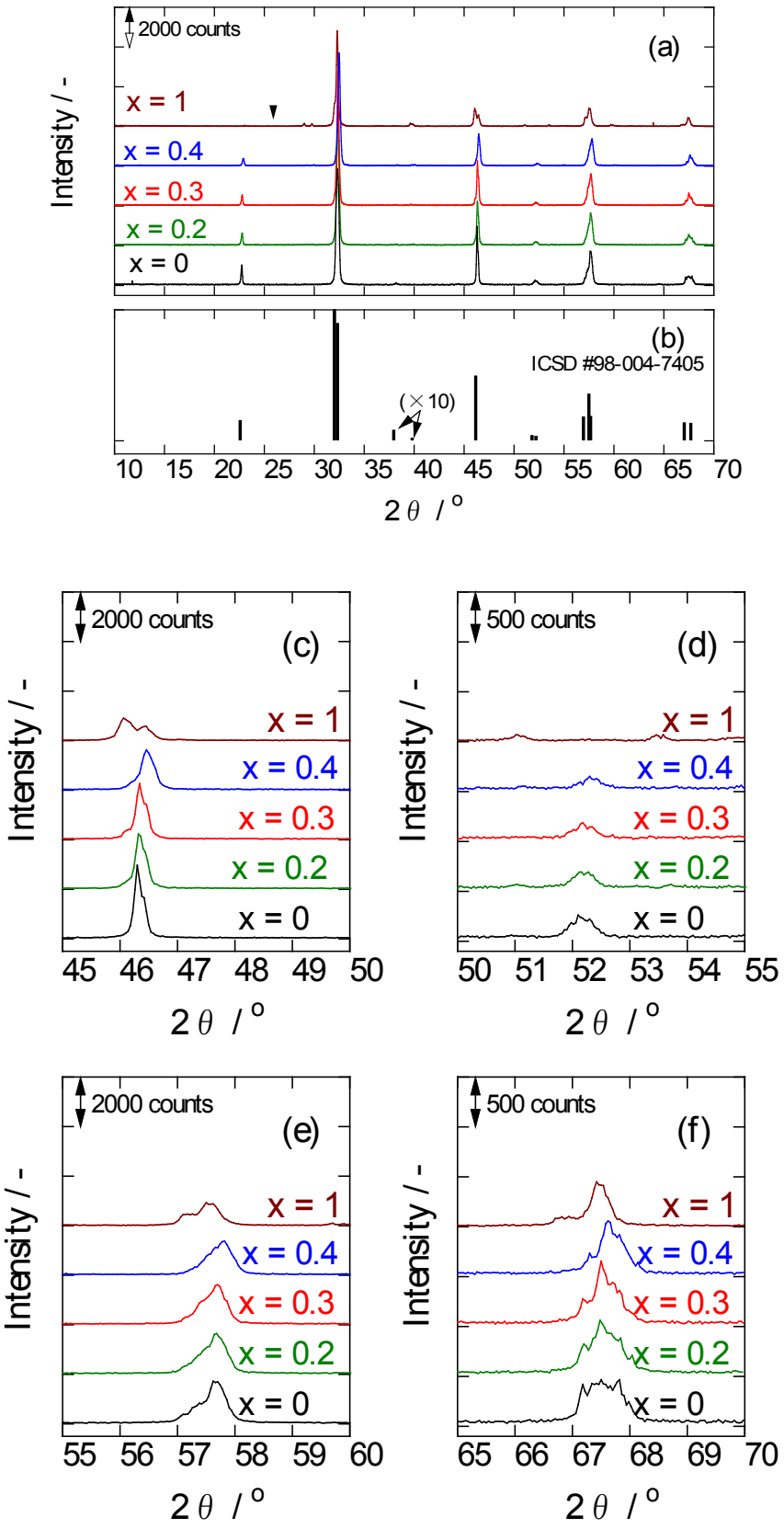

Figure S1. Observed XRD patterns of as-prepared $AgTa_{1-x}Nb_xO_3$ powders (x = 0, 0.2, 0.3, 0.4, and 1). (b) the reported XRD peaks of $AgTaO_3$ obtained from ICSD #98-004-7405. (c) – (f) are the enlargement of (a).

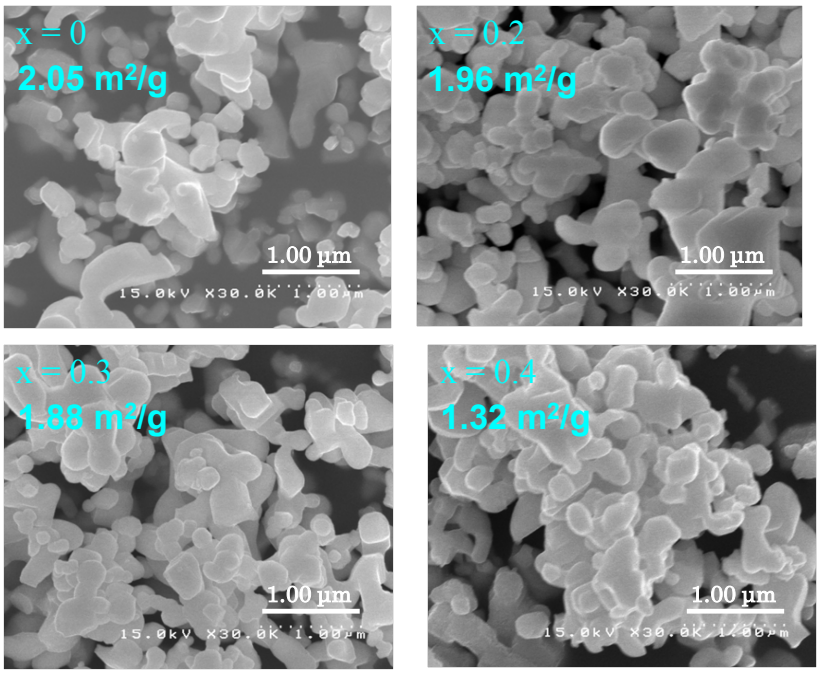

Figure S2. SEM images of $AgTa_{1-x}Nb_xO_3$ powders (x = 0, 0.2, 0.3, and 0.4, after calcination at 850 °C). The surface areas are indicated.

ESI-4) Additional explanations for the water-splitting reactions.

Wavelength distributions of the 405- and 420-nm LED sources used for irradiation are shown in Fig. 3f. The *Y*-axis was drawn using arbitrary units as the light intensities were unknown due to the specifications of the spectroradiometer (USR-40, Ushio). However, the light intensities could be speculated to be ~ 6 and ~ 40 mW/cm^2 for 405- and 420-nm LED sources, respectively. Then, we calculated the number of photons that $AgTa_{1-x}Nb_xO_3$ (x = 0.3) could absorb on irradiation from the 405-nm and 420-nm LED light sources (Table S1). We calculated the H_2 evolution rates from the slopes of the plots in Figs. 3b, 3e, and 4, and then estimated the QE values using the equation: QE = {(number of evolved H_2 molecules × 2) / number of absorbed photons} (as described by Maeda, K.; Teramura, K.; Takata, T.; Hara, M.; Saito, N.; Toda, K.; Inoue, Y.; Kobayashi, H.; Domen, K. *J. Phys. Chem. B*, **2005**, *109*, 20504-20510) (Table S1).

Table S1. H_2 generation rates under 405- and 420-nm-LED lights, normalized photon numbers and QE values in the presence of $NiO/AgTa_{0.7}Nb_{0.3}O_3$.

Light source	H_2 generation rate / μmol h^{-1}	Absorbed photon number / quanta s^{-1}	QE / %
LED 405 nm	2.0×10^{-3}	6.3×10^{17}	1.1×10^{-4}
LED 420 nm	$(8.5 \pm 1.6)\times10^{-3}$	3.1×10^{18}	$(0.98 \pm 0.19)\times10^{-4}$

As described in the Introduction section, the VB top potential of $AgTa_{0.7}Nb_{0.3}O_3$ can be assumed to be 2.5 V vs. SHE. As the LED lights with wavelengths of 405 and 420 nm have energies of 3.06 and 2.95 eV, respectively, the potentials from the VB top are estimated to be –0.56 V and –0.45 V vs. SHE, respectively.

Figure S3 shows the raw data for N_2 (open black circles), O_2 (black crosses), and H_2 (closed red circles) concentrations (denoted as obs.) and the calculated O_2 concentration (denoted as calc., closed blue circles) in the presence of $NiO/AgTa_{1-x}Nb_xO_3$ (x = 0.3) irradiated with 420-nm LED light. The calculated O_2 concentration was obtained using the following equation: O_2 (calc.) = O_2 (obs.) – (N_2 (obs.) / 0.78) × 0.21, which assumes that the "impurity" O_2 originated from external air that entered the system. In Fig. 4 in the main text, plots of O_2 concentration were calculated ones. Although it is unknown whether the "impurity" O_2 originated from the external air or from O_2 remaining in water, each time we performed the water-splitting experiments, a different amount of N_2 was detected. We repeatedly deaerated this system to a final pressure of 2.5 Pa and then introduced argon gas into the system in the same way. For this reason, we considered that the effect of residual O_2 (or N_2) might be possibly excluded. Thus, we assumed that the "impurity" O_2 originated from external air that entered the system in the present study. Notably, the amount of impurity O_2 was negligibly small. In addition, N_2 was not observed during the third and fourth cycles at all, and was observed only at the last point of the first and second cycles. Thus, we confidently concluded that the observed O_2 evolution was the result of water splitting by the photocatalyst.

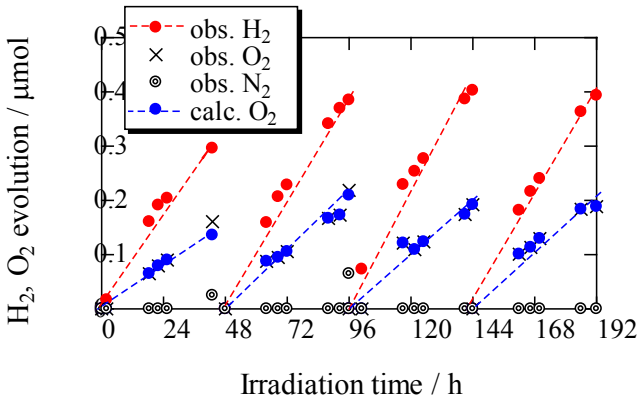

Figure S3. Raw data of Fig. 4 in the main text, N_2 (double black circles), O_2 (black crosses) and H_2 (closed red circles) concentrations (denoted as obs.). Calculated O_2 concentration (denoted as calc., blue closed circles).

To guarantee the photo-induced water splitting under visible light irradiation (420-nm and 405-nm LED lights), we evaluated the water-splitting reaction in the presence of $NiO/AgTa_{0.7}Nb_{0.3}O_3$ under the identical condition except for "without the light irradiation". In the dark with only stirring the photocatalyst powders with a magnetic stirrer, neither H_2 nor O_2 were observed as shown in Fig. S4.

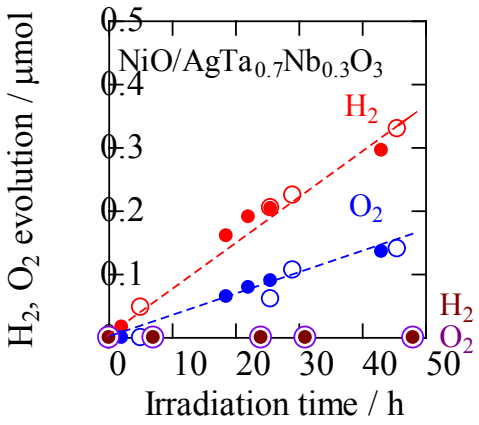

Figure S4. Time courses of H_2 (closed brown circles) and O_2 (open purple circles) amounts resulting from water-splitting test in the presence of $NiO/AgTa_{1-x}Nb_xO_3$ (x = 0.3) in the dark. Time courses of H_2 (open and closed red circles) and O_2 (open and closed blue circles) evolutions were exactly the same as those shown in Fig. 3 (b).

Figure S5 shows the results of the water-splitting tests for $NiO/AgTa_{1-x}Nb_xO_3$ (x = 0.3, 20 mg) and bare $AgTa_{1-x}Nb_xO_3$ (x = 0.3, 60 mg) irradiated with an Xe lamp. The linear generation of H_2 and O_2 with a ratio of 2 to 1 was observed in the presence of $NiO/AgTa_{1-x}Nb_xO_3$ (Fig. S5). In contrast, without grafting NiO onto $AgTa_{0.7}Nb_{0.3}O_3$, only slight O_2 evolution was observed, but H_2 was not as shown in Fig. S4. Then, it is reasonable to consider that NiO is the active site for H_2 and that the calculated H_2 turnover number is based on NiO. The prepared $NiO/AgTa_{1-x}Nb_xO_3$ contained NiO with a $NiO/AgTa_{1-x}Nb_xO_3$ weight percentage of 0.5 wt%. Therefore, the weight of NiO was 0.1 mg, which corresponds to 1.33 μmol. We confirmed that the total amount of H_2 generation was 74.9 μmol. Thus, the turnover number of produced H_2 to the total amount of NiO co-catalyst was 74.9 μmol / 1.33 μmol, equalling 56.3.

We can provide that the ternover number exceeded 1 if it was calculated based on the $AgTa_{1-x}Nb_xO_3$ (x = 0.3), as follows; 20 mg of $NiO/AgTa_{1-x}Nb_xO_3$ (x = 0.3) contains 19.9 mg of $AgTa_{1-x}Nb_xO_3$ (x = 0.3) as NiO was 0.1 mg as described above. Then, 19.9 mg of $AgTa_{1-x}Nb_xO_3$ (x = 0.3) corresponds to 61.2 μmol. Thus, the turnover number of produced H_2 to the total amount of $AgTa_{1-x}Nb_xO_3$ (x = 0.3) was 74.9 μmol / 61.2 μmol, equalling 1.22.

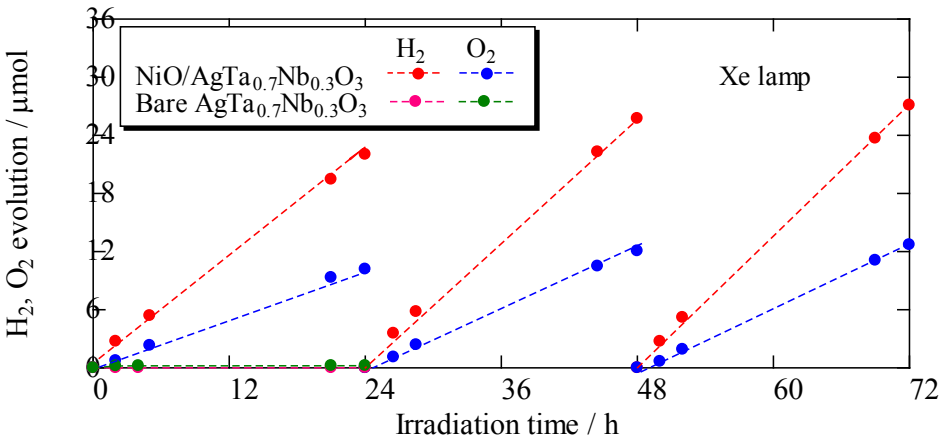

Figure S5. Time courses of H_2 and O_2 evolutions resulting from water-splitting in the presence of $NiO/AgTa_{1-x}Nb_xO_3$ (x = 0.3) and bare $AgTa_{1-x}Nb_xO_3$ (x = 0.3) irradiated with the Xe lamp without any optical filters.

Ag^+-containing photocatalyst always raises a question about Ag^0 formation as a reduction product of Ag^+. So, using an X-ray photoelectron spectroscopy (XPS, JPS-9200, JEOL), Ag 3d spectrum of the $NiO/AgTa_{1-x}Nb_xO_3$ (x = 0.3) photocatalyst under Xe light irradiation was confirmed. The photocatalyst after 72 h light irradiation in Fig. S5 was collected and served for the measurements. Ag 3d XPS spectrum was unchanged after light irradiation, compared to that before light irradiation (Fig. S6). So, Ag^+ in the present $NiO/AgTa_{1-x}Nb_xO_3$ (x = 0.3) was quite stable under the present light condition. This would be caused by the HNO_3-treanment of the photocatalyst, which removed the remaining Ag species on its surface.

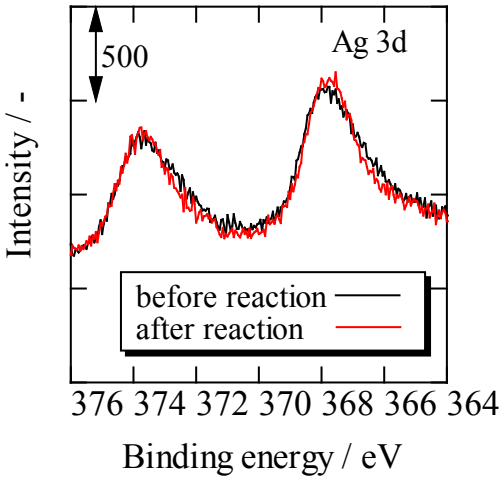

Figure S6. Ag 3d XPS spectra before (black) and after water-splitting reaction (red) of $NiO/AgTa_{1-x}Nb_xO_3$ (x = 0.3).

We examined the evolution of H_2 and O_2 from pure water in the presence of $NiO/AgTaO_3$ under light irradiation of > 560 nm (Figure S7a). Then, neither H_2 nor O_2 were observed at all (Figure S7b). Note that N_2 was not observed during this period at all. Thus, we could confidently conclude that the H_2 production did not occur by the light absorption around 600 nm.

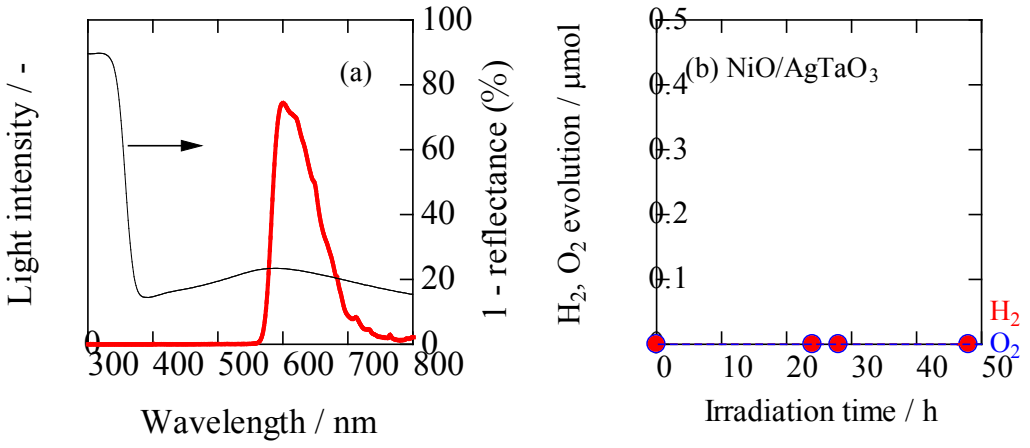

Figure S7 (a) Wavelength distribution of the irradiated light is shown. The light intensity is unknown due to the specifications of the spectroradiometer (Xe lamp + a combination of Y-44 and O-58 glass filters). UV-visible absorption spectra of bare $AgTaO_3$ is also shown. (b) Time courses of H_2 (closed red circles) and O_2 (open blue circles) amounts resulting from water-splitting test in the presence of $NiO/AgTaO_3$ under > 560 nm light irradiation as shown in (a).